ELSEVIER

International Journal of Mass Spectrometry 203 (2000) 111–125

International Journal of Mass Spectrometry

# Significant interferences in the post source decay spectra of ion-gated fullerene and coalesced carbon cluster ions

Mark P. Barrow, Thomas Drewello*

*Department of Chemistry, University of Warwick, Coventry CV4 7AL, England, UK*

Received 10 July 2000; accepted 14 July 2000

**Abstract**

Post source decay experiments have been performed with fullerene radical cations and large carbon cluster radical cations, produced from laser desorption/ionization and studied by applying reflectron time-of-flight mass spectrometry. Utilising the wide-spread technique of continuous ion extraction, in conjunction with a deflecting electrode (ion gate) for the selection of ions, the experimental method is carefully evaluated in light of the observation of interfering, artefact signals which have been established as resulting from delayed ionization of fullerenes. (Int J Mass Spectrom 203 (2000) 111–125) © 2000 Elsevier Science B.V.

*Keywords:* Fullerenes; Coalescence; Post source decay; Delayed ionization; Laser desorption/ionization; Reflectron time-of-flight mass spectrometry

## 1. Introduction

Not only does the presence of an ion mirror (reflectron) in the linear flight tube increase the resolving power, but it also paves the way for tandem mass spectrometry experiments. Daughter ions generated after acceleration continue to move with the same velocity as their parent ions, resulting in the same arrival time at the end of the linear flight tube. Due to the difference in mass, daughter ions will possess a lower kinetic energy than the parent ion, and so the two ions penetrate the electric field in the reflectron to different extents. The distinct residence times in the reflectron therefore give rise to distinctive arrival times at the final detector, hence daughter and parent ions may be resolved in a reflectron time-of-flight (TOF) instrument. The fragmentation of ions in the field free region of the flight tube is referred to as post source decay (PSD) [1–3]. Post source decay features prominently in the structure elucidation of molecular ions derived from matrix-assisted laser desorption/ionization (MALDI) [4,5]. As a means of gaining structural information via interpretation of the fragmentation pattern, PSD represents an important tandem mass spectrometry experiment. The competitiveness with other tandem mass spectrometry (MS/MS) experiments, such as high energy collision-induced dissociations (CID) applying multisector instruments, appears to be an issue. Critical features [1,2] in PSD experiments include the accuracy of the daughter ion mass assignment, the daughter ion resolution and the

* Corresponding author. E-mail: t.drewello@warwick.ac.uk


*PII* S1387-3806(00)00293-1

parent ion selectivity as achieved by utilising an ion gate for the precursor ion selection.

This report covers PSD experiments with fullerene cations produced from laser desorption/ionization (LDI) and giant carbon cluster cations originating from laser-induced coalescence reactions. Although laser ablation of graphite led to the discovery of fullerenes [6], laser ablation of fullerenes was found to result in the formation of large carbon clusters [7]. The latter coalescence reactions produced enhanced signals for the carbon cluster cations close to the multiples of the initial fullerene mass. It was found that coalescence occurs even without the use of a buffer gas, which was originally employed [8,9], and that the formation of anionic species can be as efficient as the cation production [9]. Important contributions to the understanding of the underlying mechanism of coalescence reactions and the structural features of the resulting carbon moieties are currently obtained by a variety of different approaches. These include, for instance, the examination of structure-indicative arrival time distributions in ion chromatography experiments [10–13], the analysis of fusion products derived from LDI of deliberately modified carbon cores [14–17] and investigations into the delayed ionization of coalesced carbon clusters [18,19].

Only a few investigations are concerned with the fragmentation behaviour of size-selected large carbon cluster ions, and the performance of high energy CID of ions derived from LDI represents a challenge to instrumentation [20]. During a recent investigation into the CID of fullerene ions [21], generated by MALDI while analysing $C_{70}^{+\cdot}$, a tremendous degree of scattering was encountered when choosing larger target gases (in order to reach a favourable centre-of-mass collision energy region). In the following, experimental findings are discussed, which were initially aimed at the utilization of PSD as a possible means to fragment large carbon cluster ions. The results reveal that significant interferences can obscure the PSD spectra, which in turn can easily lead to incorrect interpretation. The artefacts observed are attributed to the delayed ionization of the carbon clusters.

## 2. Experiment

The experiments were conducted using a commercially available reflectron time-of-flight mass spectrometer (Kompact MALDI IV, Kratos, Manchester, UK) of which the essential parts for this investigation are depicted in Fig. 1. This setup has recently been successfully applied to a variety of laser-induced coalescence [14,22] and aggregation reactions [23].

For LDI, the instrument is equipped with a nitrogen laser operating at 337 nm with a pulse length of 3 ns. Ions are accelerated by a continuous potential difference of 20 kV, maintained between the stainless steel sample holder and a grid which was maintained at earth potential. The length of the acceleration region is 12 mm. The laser pulse triggered the start of each flight time measurement. A deflecting electrode is located at a distance of 200 mm from the sample holder further down the linear flight tube operating as the ion selecting device, or “ion gate.” The ion gate employs a potential to deflect all arriving ions; it is switched off at times when the temporal positions of the ions to be selected coincide with the physical position of the ion gate. At all other times, during the course of experiments that make use of the ion gate, the ion gate is switched on. In this manner, an ion of a chosen mass, or ions over a chosen mass range, may be selected in order to obtain a PSD spectrum. Such a spectrum consists of signals from the selected ions and daughter ions arising from fragmentation in the field free region of the flight tube. A curved field reflectron [24] of 370 mm length is positioned at a distance of 160 mm after the ion gate. The curved field reflectron focuses all daughter ions onto the detector so that, in contrast to other types of ion mirrors, no stepping of the reflectron potentials is required in order to observe all daughter ions, nor is any variation of the laser power required during a particular experiment. The instrument is controlled using a Sun Sparc workstation, running the KOMPACT V5.1.2 program. The width of the ion gate is variable and can also be used in MALDI to suppress matrix signals by “blanking” out low mass signals, while allowing all ions of higher mass to pass. It is clear that the physical dimensions of the gate and its operation

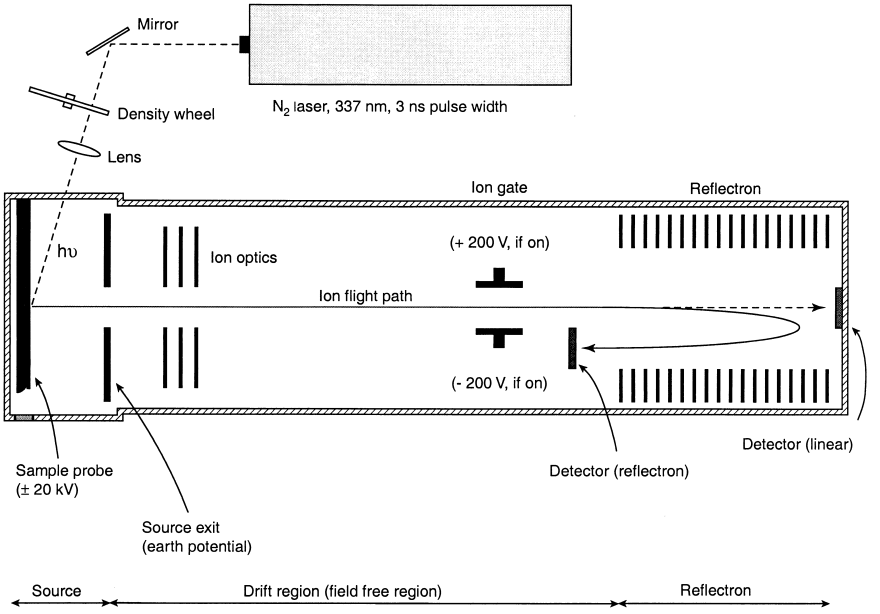


Fig. 1. Schematic diagram of the instrumental design of the Kratos Kompact MALDI IV.

determine the resolving power and thus the selectivity that can be achieved.

Since a measure of the selectivity of the ion gate is of essential importance for the following, the ion gate was tested performing MALDI in the positive ion mode with poly(ethylene glycol) of the average molecular weight, $M_n = 1000$ (PEG 1000). The technical specification for the ion gate of this instrument correlates to the use of PEG 1000 as the calibrant. It states that when the most intense peak is selected, three oligomers should reach the detector, with the "outer" two peaks having an intensity of 10% of the central, selected peak. Fig. 2(a) shows the obtained distribution of polymer ions formed by metal ion attachment, which are spaced by 44 Da. In Fig. 2(b) the result of gate-selecting the ion with *m/z* 1010 is shown. In addition to the selected ion, a small contribution at *m/z* 966 is observed. This ion may be a fragment arising from PSD or it may be an ion passing through the ion gate, due to the uncertainty associated with the gate accuracy. No signal, however, is observed at *m/z* 1054. From this result, it can be seen that in this mass range the selectivity of the ion gate for ions of equal abundance is approximately ±44 Da. Although this selectivity is poor, it is perfectly sufficient to lead the argument in the following discussion.

The fullerene samples were of commercial origin (Southern Group Chemicals [$C_{60}$ and $C_{70}$] and CarboTech [$C_{84}$]). The fullerenes were deposited onto a stainless steel target slide in the form of a toluene solution and dried in a cold air stream before introduction into the ion source. Each individual TOF mass spectrum shown here represents the accumulation of 100–200 "profiles" or "laser shots."

## 3. Results and discussion

The LDI mass spectrum derived from a pure $C_{60}$ target is shown in Fig. 3(a). The signal of the $C_{60}^{+\cdot}$ cation radical is accompanied by the well-known fragment ion pattern, which is, in accordance with earlier photoionization studies [25], characterised by the loss of intact, even numbered carbon units. This is interpreted in conjunction with electron impact induced, unimolecular fragmentation as a consequence of successive $C_2$ losses [26]. The high mass region is

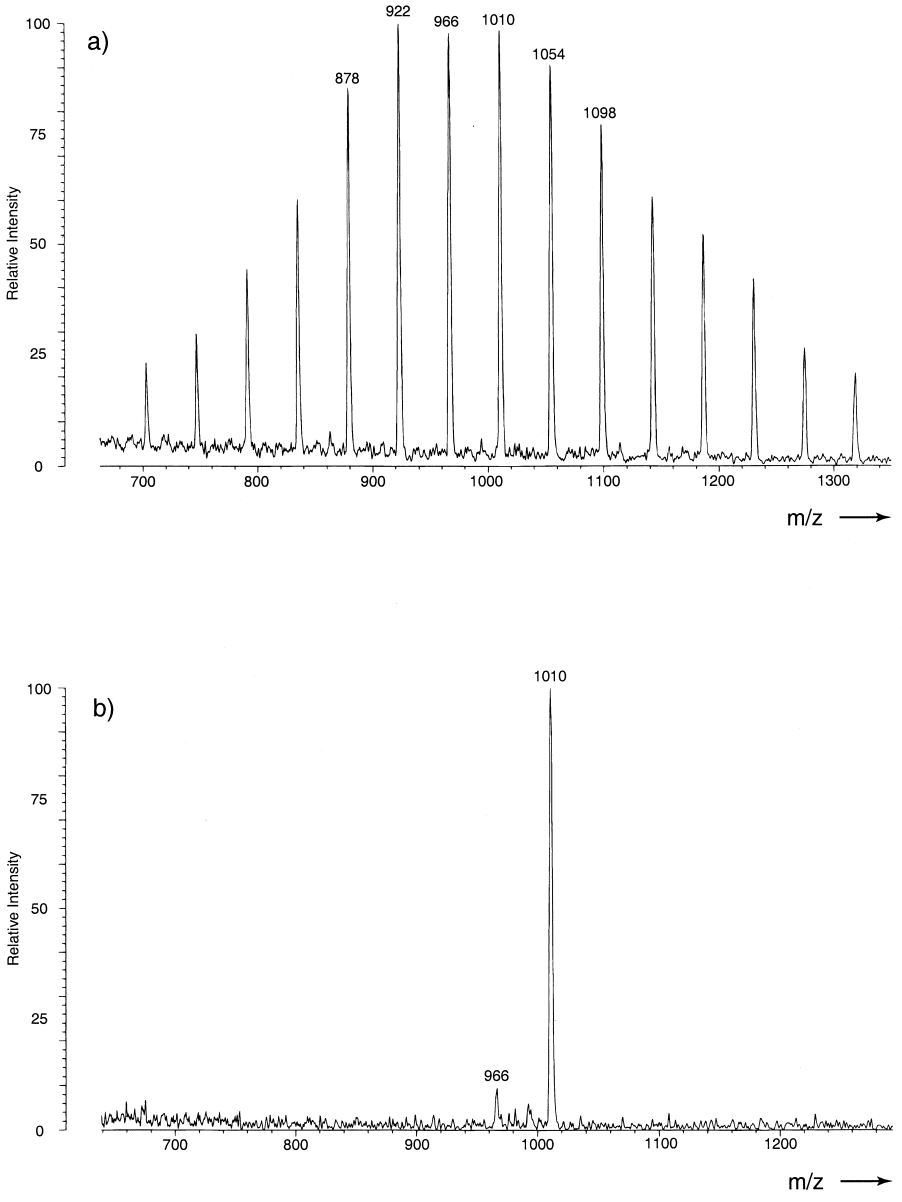


Fig. 2. MALDI mass spectra of PEG 1000 to test the selectivity of the ion gate. (a) Normal mass spectrum, with an even spacing of 44 Da existing between the signals. (b) Ion gate is set to pass *m/z*1010. Note the small trace from *m/z*966.

characterised by the presence of giant carbon cluster ions which are formed in coalescence reactions, taking place in the expanding plume of the ablated, energized target material. The mechanistic understanding of these laser-induced coalescence reactions is of intense current research interest [14–17,19]. During the course of these investigations, issues such as the importance of precursor fragmentation [27], the role of the $C_2$ density in the plume [7] and the dependence on the target material [14–17] have been critically addressed. Closely connected with mechanistic questions is the elucidation of the structures of

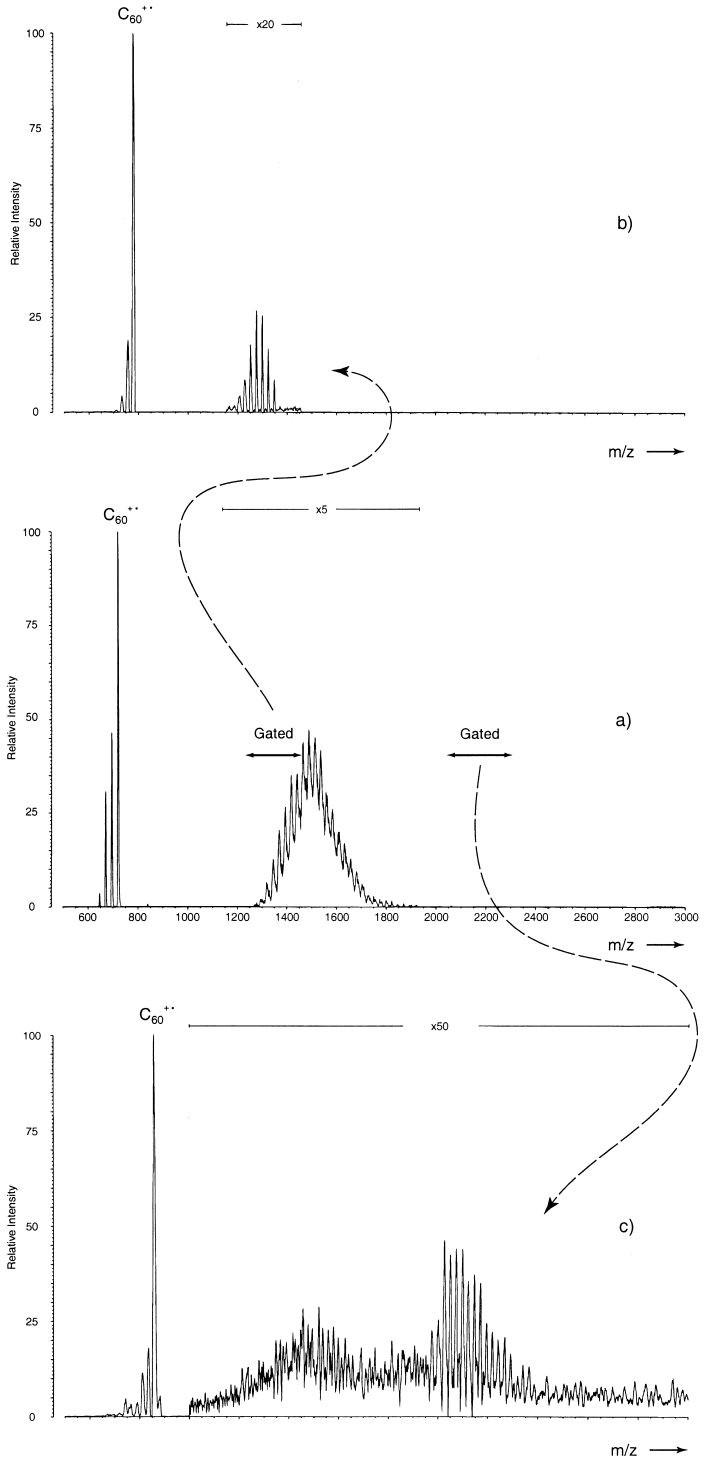


Fig. 3. LDI mass spectra resulting from $C_{60}$. (a) Normal mass spectrum. (b) PSD spectrum after gating indicated dimer region. (c) PSD spectrum after gating the indicated trimer region.

coalesced clusters. Surface-induced dissociation of $C_{120}^{+\cdot}$ resulting from coalescence of $C_{60}$ shows no indication of a $C_{60}^{+\cdot}$ fragment ion [7], which seems to support a closed-cage, fullerene-like structure. However, recent ion mobility studies reveal the existence of at least one additional isomer with dumbbell geometry [28], in which two intact $C_{60}$ moieties are covalently bound to each other. In this context, the post source decay experiment might be a valuable, alternative tool to obtain structural information via the fragment ion analysis of gate-selected precursor ions.

The PSD spectra obtained using ion gate settings chosen to select precursor ions of the mass range indicated in Fig. 3(a), are shown in Fig. 3(b) and (c), thereby including carbon clusters from the dimer and trimer region of coalesced $C_{60}$, respectively. For both of these PSD spectra, the gate width is chosen to allow several precursor ions of different masses to pass in order to improve the fragment ion abundances. The PSD spectra are presented as plots of the relative intensity versus mass-to-charge ratio. Crucial to the assignment of the daughter ion masses is the translation of the measured TOF into a mass scale. Several methods exist to achieve this goal [2], including ion flight time simulations and calibration procedures which mathematically correlate the flight time of precursor and fragment ions of the same mass with each other. In favourable cases, even internal calibration can be applied, in which the assignment of the unknown daughter ions is achieved by relating their flight time to the appearance of well-known fragment ions in the same spectrum. At first sight this latter approach seems to be perfectly applicable in the present case. Since the spacing between all neighbouring fragment ions is entirely due to loss of a $C_2$ moiety, a simple count down from the selected parent ions of known masses would allow the establishment of the composition of the carbon cluster ions causing the signals in the spectra depicted in Fig. 3(b) and (c). Application of this method reveals that the base peak in both PSD spectra undoubtedly results from $C_{60}^{+\cdot}$. In Fig. 3(c), the characteristic fragmentation pattern can be observed with an enhanced $C_{60}^{+\cdot}$ signal. In other words, the PSD spectra seem to imply that, besides the expected $C_2$ losses, the most prominent dissociation channel leads to the $C_{60}^{+\cdot}$ fragment ion. The structural implications drawn from this would result in the assumption that a considerable fraction of the selected carbon cluster population possesses geometrical features closely related to a dumbbell geometry, with the $C_{60}$ unit possibly retained. The appearance of the spectrum shown in Fig. 3(c) would be in line with such an assumption. Ions of the trimer region, composed of three isolated carbon cage moieties, could fragment into dimeric species, which in turn could dissociate to form the $C_{60}^{+\cdot}$ fragment ion. These conclusions, however, would be in direct contradiction to the findings cited in the literature [7,14–17]. In order to evaluate the influence of the target material, the precursor fullerene for the coalescence reactions is varied.

The PSD spectra obtained for gate-selected ions of the dimer region of $C_{60}$, $C_{70}$, and $C_{84}$ are depicted in Fig. 4(a)–(c), respectively. The shaded peaks represent the precursor ions, which are selected by the ion gate. The most striking feature of this comparison is the fact that these PSD spectra strongly suggest that the precursor fullerene of the gate-selected giant carbon cluster is re-generated in the dissociation. Thus, one might possibly assume that the giant carbon clusters of the dimer region still retain structural elements that are closely related to the fullerene precursor involved in the coalescence reaction. However, a careful analysis of the overall appearance of the PSD spectra presented so far reveals a number of features that make it very unlikely that the signals obtained actually originate from the fragmentation of the selected larger clusters. The intensity patterns obtained in Fig. 4(a)–(c) are so characteristic for the respective fullerene, that there can be no doubt that the signals represent in fact the species to which they are assigned. However, the relative intensity with which these signals appear in relation to the precursor ion abundances is in fact most unexpected, for two reasons. The first reason is that the intensity patterns for the respective fullerenes closely resemble the fragmentation pattern observed in a normal mass spectrum for the respective fullerenes, which is observed when using a low laser fluence. The second reason is that in all of the PSD spectra, the assumed,

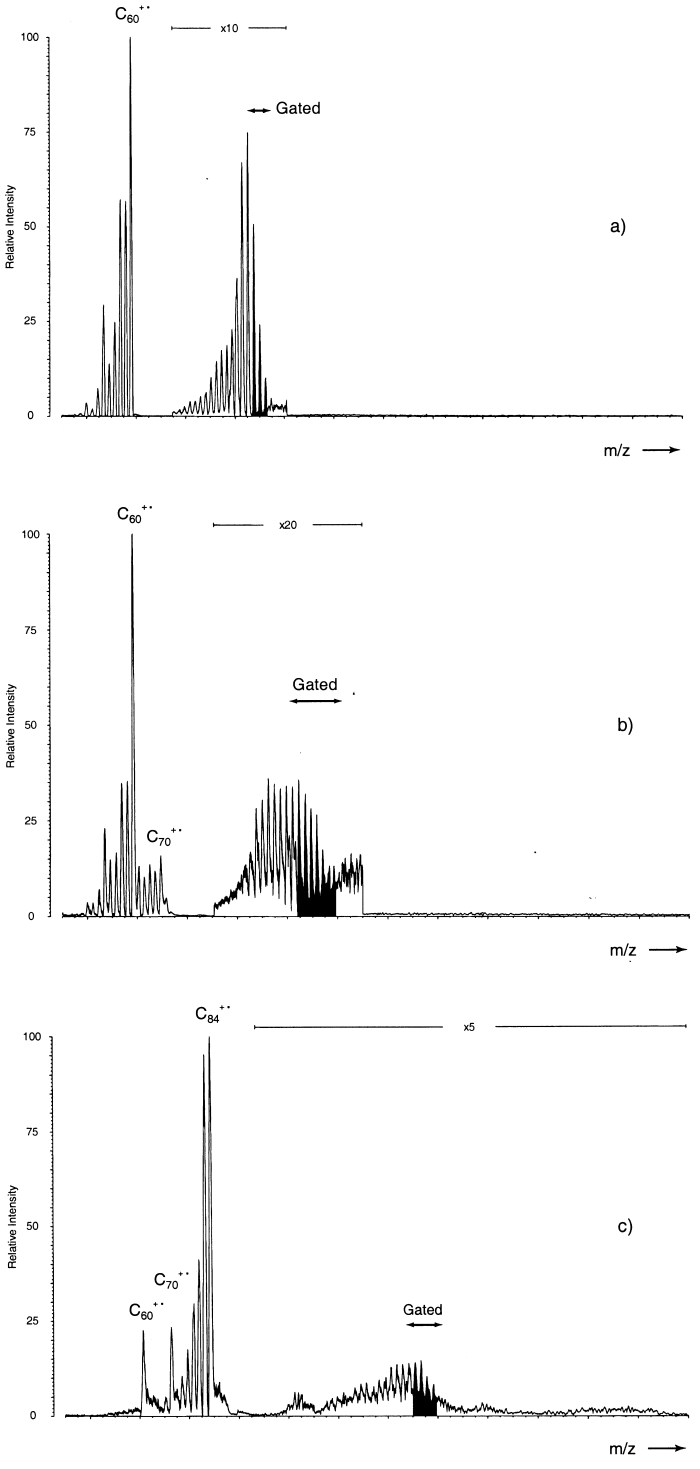


Fig. 4. Comparison of PSD spectra of the dimeric species formed by LDI using three different target materials. (a) PSD spectrum resulting from gating the dimeric species formed by LDI of $C_{60}$. (b) Same as (a) but using $C_{70}$ instead of $C_{60}$, and (c) Same again but using $C_{84}$.

monomeric fragment ion is tremendously more abundant than the selected parent ion. Even when considering relatively weak attractions operating in the precursor species the assumed fragment ion appears far too abundant, and, as stated earlier, the evidence for such coalesced carbon cores existing as closed, fullerene structures instead of dumbbell-shaped structures has become very strong indeed. The coalesced carbon cores should therefore not dissociate preferentially to the precursor species, but instead would fragment via the loss of $C_2$, a well-known and identifying characteristic of fullerenes. Furthermore, when the mass scale of the PSD spectra is calibrated utilising a scale based on known fragment-to-parent ion mass correlation, the assumed fragment ion signals appear at mass-to-charge ratios that are far too high (shifts ranging from several atomic mass units to approximately 300 u have been observed, depending on the conditions applied). Thus, the signals observed in the PSD spectra do not originate from the post source decay of the selected parent ion.

In the following, experiments are discussed which are aimed at the determination of the origin of these artefact peaks. In Fig. 5(a) the PSD spectrum of gated $C_{84}^{+\cdot}$ ions is shown, resulting from LDI of a pure $C_{84}$ target. The shaded peak represents the selected parent ion. The spectra shown in Fig. 5(b) and (c) are obtained under identical conditions with the exception of the target material from which the $C_{84}^{+\cdot}$ precursor was obtained. The spectra depicted in Fig. 5(b) and (c) result from $C_{84}$ targets which are doped with $C_{60}$ and $C_{70}$, respectively. As has been discussed in the experimental part (Fig. 2), the precursor ion selection with the ion gate is affected by an uncertainty which is in the region of $\pm 44$ u, so that the signals corresponding to $C_n^{+\cdot}$ with $n = 82$, 80, and possibly 78, are mainly due to stable ions that pass the gate together with $C_{84}^{+\cdot}$. However, the gate would clearly prevent the passage of $C_{60}^{+\cdot}$ and $C_{70}^{+\cdot}$ ions which leave the acceleration region at the same time as the selected $C_{84}^{+\cdot}$ ions. A likely explanation for the abundant occurrence of $C_{60}^{+\cdot}$ and $C_{70}^{+\cdot}$ ions in the spectra of Fig. 5(b) and (c), would be that these ions are not leaving the acceleration region at the same time as $C_{84}^{+\cdot}$, but later, so that their arrival time at the ion gate coincides with the arrival time of the parent ion that is selected. If the kinetic energies were equal for all ions leaving the source at any time, due to their higher velocities, the $C_{60}^{+\cdot}$ and $C_{70}^{+\cdot}$ ions would, on continuing the flight after passing the ion gate at the same time as $C_{84}^{+\cdot}$, reach the reflectron detector at shorter flight times than the selected parent ion, interfering with the appearance of the PSD spectrum. The most probable prerequisite for the interfering ions to leave the acceleration region later than the selected ions is an ability to ionize after a time delay following excitation. In fact, as one of the many fascinating properties of fullerenes, delayed electron emission [18,19,29–37] is found to play a dominant role in their ionization dynamics.

The electronic mechanism behind delayed electron emission from fullerenes is currently under intense investigation. The time domain in which delayed ionization of fullerenes can take place, and which extends into the microsecond timeframe for most experiments, is strongly dependent on the method of excitation and on the fullerene itself. Besides the period of time in which a fullerene can undergo delayed ionization, the important parameters that influence the probability of interference from these delayed ions are: the ions' velocities (dependent upon the accelerating potential and the mass of the ion) and temporal positions and the width of the ion gate. Not only the abundance of interfering ions, but also their positions in the PSD spectrum obtained depend on the flight times of all the ions involved in the PSD experiment. During the course of each profile obtained (summed to result in the final spectrum), neutral fullerene species will be ablated from the surface of the target after each laser pulse. These neutrals then move through the source towards the source exit (although some angular spread will also occur), and exist as excited neutrals for a finite period of time on a microsecond timescale. The position at which these neutrals ionize in the acceleration region will determine their translational energy. As an example, a neutral $C_{60}$ that travels in the present setup through the source at an initial velocity of approximately $10^3$ ms$^{-1}$ (a common magnitude for the initial velocity of laser ablated ions [38], neutrals often

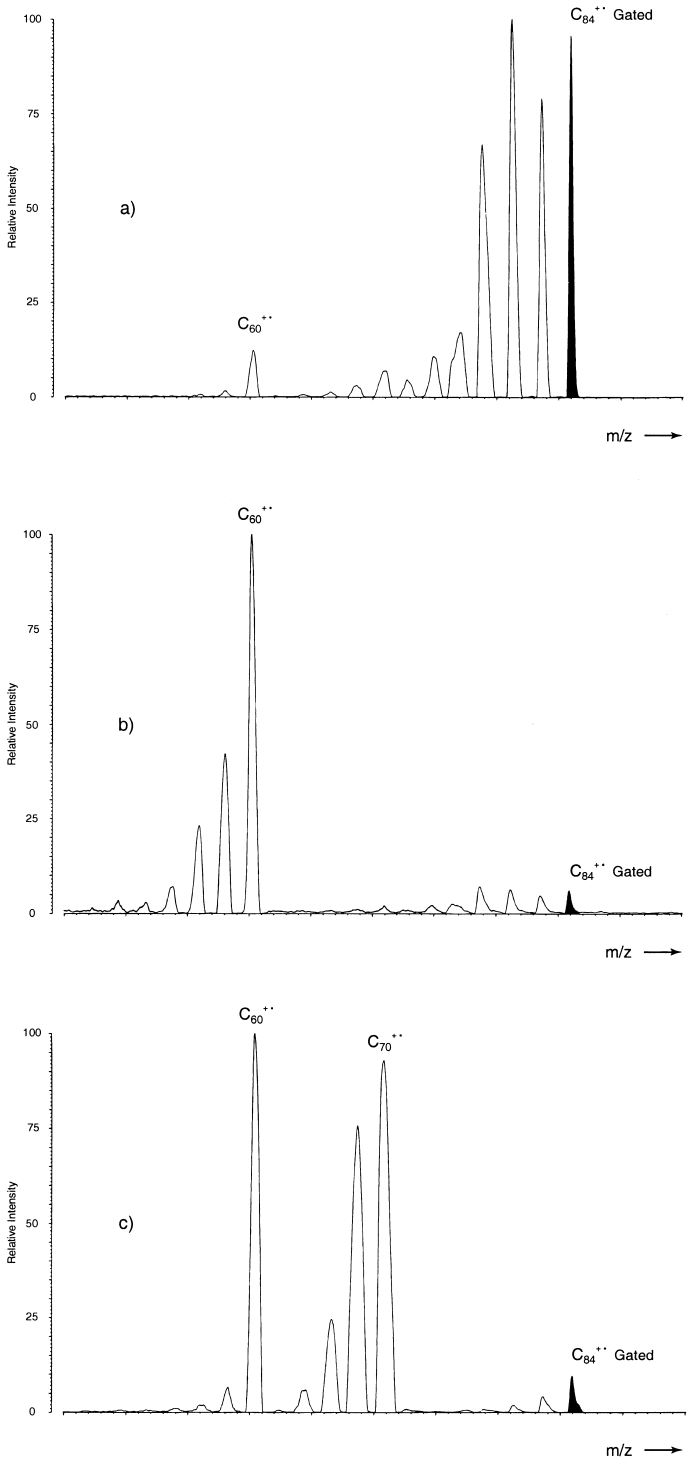


Fig. 5. Three PSD spectra, where $C_{84}^{+\cdot}$ is the gated species in each case. (a) PSD spectrum of pure $C_{84}$. (b) PSD spectrum of $C_{84}$ spiked with $C_{60}$. (c) PSD spectrum of $C_{84}$ spiked with $C_{70}$.

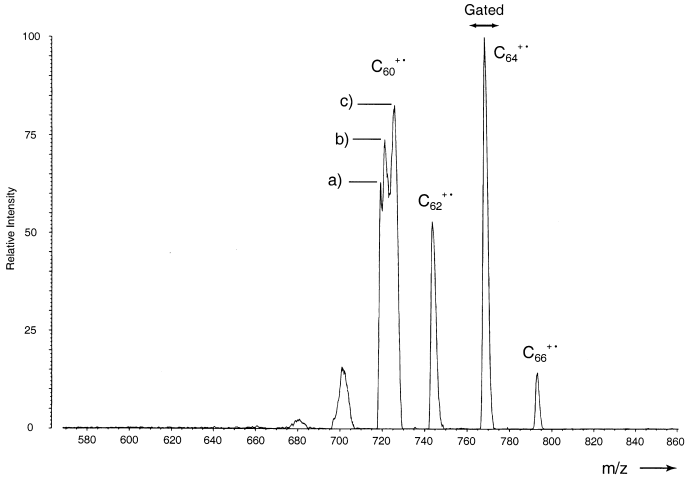


Fig. 6. Partial PSD spectrum of gated $C_{64}^{+\cdot}$ as generated from a $C_{70}$ target, showing the $C_{60}^{+\cdot}$ signal split into three components.

possess lower initial velocities [39]), would be able to pass the ion gate after ionization had occurred at a position in the acceleration region that would provide the ion with a kinetic energy of 18.2 keV, rather than the full 20.0 keV. However, in order for the neutral to travel this far in the acceleration region a delay in ionization of ~1.1 $\mu$s would be needed. Calculations performed in the course of this study clearly show that an explanation based purely on an energy deficit alone cannot explain the observations. The most important reason for this is that in order to produce a significant energy spread in the first place, delayed ionization must be a prerequisite in order for neutrals to reach positions of much lower potential in the source prior to ionization.

An illustrative example indicating the various contributions to an assumed PSD signal is shown in Fig. 6, which represents the PSD spectrum of $C_{64}^{+\cdot}$ generated from a $C_{70}$ target. The supposed fragment ion signal of $C_{60}^{+\cdot}$ clearly shows three distinct components, which are assigned by analysis of the TOF measured for the three peaks. For a given acceleration voltage, the ion velocities determine the flight time to reach the detector. The measured flight times at the peak centres for $C_{66}^{+\cdot}$, $C_{64}^{+\cdot}$, $C_{62}^{+\cdot}$, and component (a) of the $C_{60}^{+\cdot}$ signal have revealed that these peaks are due to source-generated ions caused by prompt ionization. These ions pass the ion gate as the result of its poor resolving power. The signals resulting from $C_{60}^{+\cdot}$ due to delayed ionization, however, would be shifted as a delay in ionization is needed for the faster moving $C_{60}^{+\cdot}$ to reach the gate at the same time as the gate-selected, heavier (and thus slower moving) ion. In this case, the selected ion is $C_{64}^{+\cdot}$. As stated previously, an energy spread of ions produced through delayed ionization will also be evident and result in broadened peaks, but the greatest component of the added flight time arises from the delay in ionization itself. The measured time difference between the peak components (a) and (c) in associated with a difference in total flight time needed for $C_{60}^{+\cdot}$ to jointly arrive with the $C_{64}^{+\cdot}$ ion at the physical location where the ion gate is situated in the flight tube. Thus, evidence is provided that the peak component (c) is in fact the result of $C_{60}^{+\cdot}$ formed by delayed ionization. The exact assignment for the peak component (b) cannot be established beyond doubt. It is clear, that if the selectivity of the ion gate is not sufficiently high to prevent the promptly ionizing $C_{60}^{+\cdot}$ ions from passing, $C_{60}^{+\cdot}$ ions produced through delayed ionization will pass as well, with the greatest transmission occurring when the gate is fully open. Therefore, a contribution to component (b) will also result from delayed ionization of $C_{60}^{+\cdot}$, where the gate is neither fully open or fully closed. Another likely contribution to component (b), however, can be

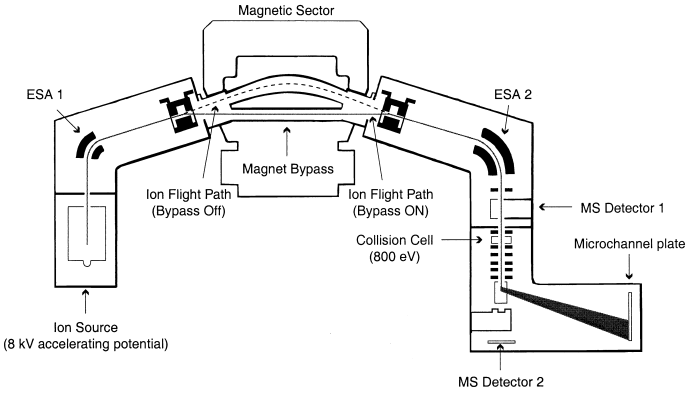


Fig. 7. Schematic representation of the Micromass AutoSpec-oaTOF mass spectrometer.

post source decay of $C_{62-66}^{+\cdot}$ ions passing the gate, resulting in the formation of $C_{60}^{+\cdot}$.

Finally, experiments are described which provide further indications that the giant carbon clusters discussed in this article are not likely to undergo an abundant fragmentation into the initial "monomeric" fullerene. In the course of investigations into the LDI behaviour of fullerene derivatives applying high resolution mass spectrometry, an AutoSpec-oaTOF, [40] as shown in Fig. 7, was utilised at Micromass Ltd. (Altringham, UK) and the results will be published in a forthcoming article [41]. In the present study, this instrument was applied to conduct collision-induced dissociations (CID) of "dimeric" carbon cluster cations derived from LDI of $C_{70}$ under conditions identical to those discussed for the reflectron time-of-flight (ref-TOF) experiments. The AutoSpec-oaTOF consists of an $E_1$–$B$–$E_2$–oaTOF configuration ($E$ denotes electrostatic sector, $B$ stands for magnetic sector and oaTOF represents an orthogonal time-of-flight analyser). Ions were derived from LDI using a nitrogen laser, as used during experiments performed on the Kompact MALDI IV, and the ions were then accelerated by a static accelerating potential of 8 kV. After the passage through the first three sectors, ions are decelerated to a laboratory translational energy of 800 eV to allow collision-induced dissociations under multiple collision conditions with a collision gas, which was xenon in the present case. The collision cell precedes an acceleration chamber in which a short pulse is applied in order to push the ions leaving the collision cell into the orthogonal TOF analyser to allow for daughter ion analysis. Using the magnetic sector, it is possible to select isotopically pure carbon cluster ions that are free from any interferences arising from delayed ionization or which result from unimolecular fragmentation during the flight through the instrument. However, the ion abundances of the large carbon clusters selected in this way were too weak to provide an efficient fragmentation pattern. Therefore, CID experiments were conducted "bypassing" the magnet. In these experiments the ion beam is directed through a second flight tube (bypass), which is located outside the magnet and which converts the instrument into a large scale tandem TOF mass spectrometer consisting of the orthogonal TOF analyser which is now preceded by a linear flight tube that passes through $E_1$ and $E_2$, bypassing the magnet. After the collision event, the acceleration electrode pushes the ion beam into the orthogonal TOF analyser with a 4% mass spread. Thus, the dissociations of all major carbon clusters in the dimer region can be sampled giving rise to a better signal-to-noise ratio for the resulting daughter ions. In this way the dissociations of the clusters covering approximately the mass range from $C_{126}$ to $C_{132}$ were sampled.

Fig. 8(a) shows the corresponding partial LDI spectrum of $C_{70}$ in the absence of a collision gas, with the dimer species clearly observable at $m/z$ 1680. Fig. 8(b) shows the same species but under CID conditions, using xenon as the collision gas. Although these clusters underwent efficient dissociations due to the

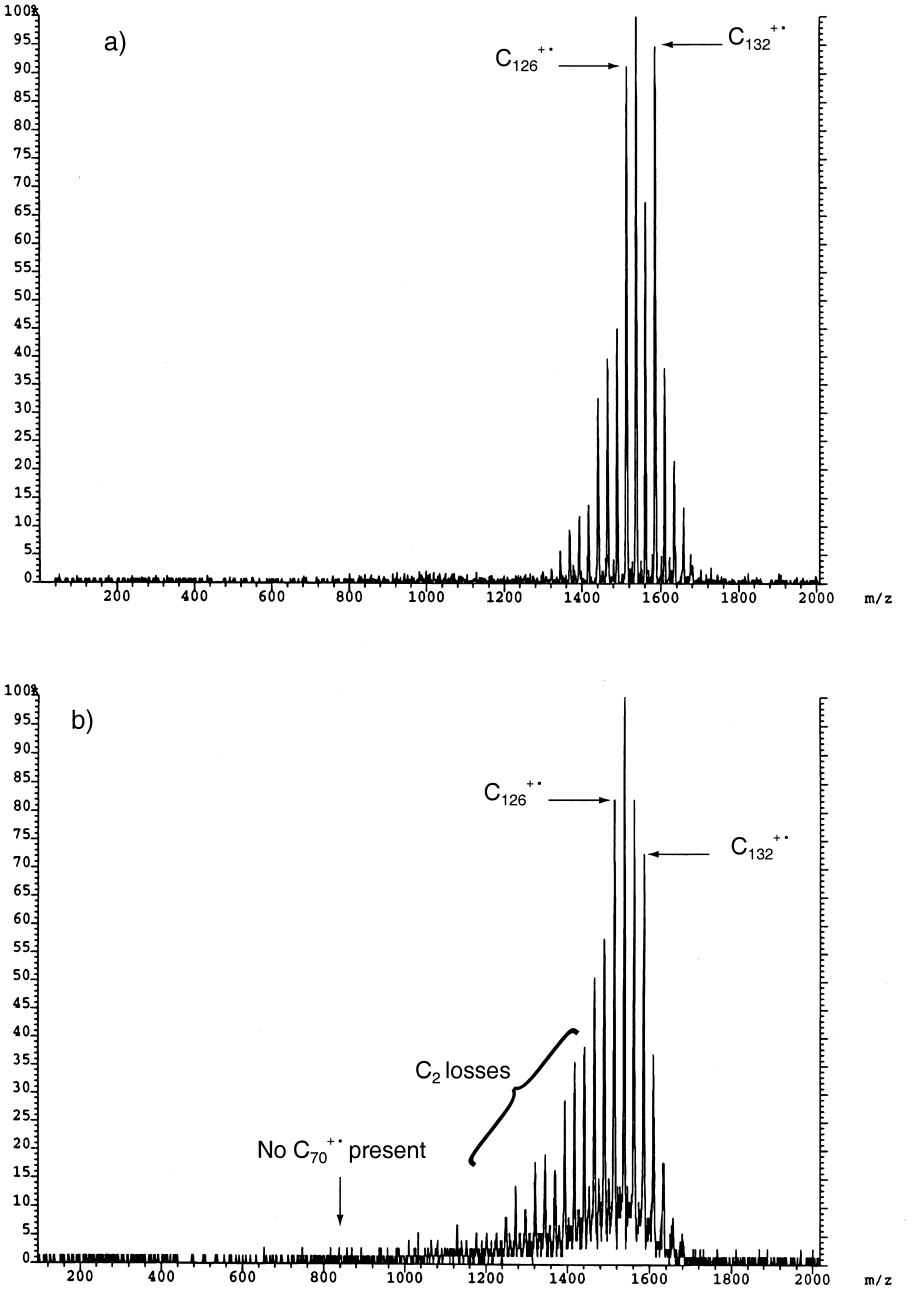


Fig. 8. Tandem TOF mass spectrum of coalesced ions derived from $C_{70}$ using the bypass option of the AutoSpec TOF and covering precursor ions of approximately $C_{126-134}^{+\cdot}$. (a) No collision gas and (b) multiple CID at 800 eV with Xe.

formal loss of several $C_2$ units, no sign of a $C_{70}^{+\cdot}$ daughter ion, resulting from PSD or CID, could be obtained under these conditions. This fragmentation pattern possibly resembles closely what can be expected from interference-free PSD spectra. Although the actual mechanism by which the ion activation

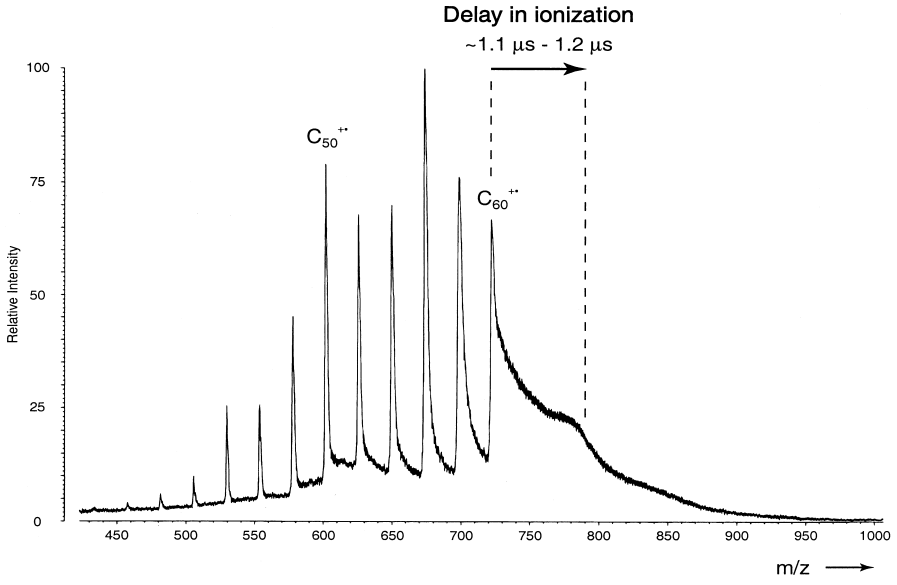


Fig. 9. LDI mass spectrum of $C_{60}$ obtained with the Kratos Kompact MALDI IV, showing the tail as the result of delayed ionization. No processing was carried out on the data.

occurs in PSD experiments is not yet understood in much detail and may be regarded as activation resulting from a combination of laser light, collisional activation in the expanding plume and by collisions occurring in the flight tube, comparative PSD and CID studies [42,43] revealed a close resemblance of PSD spectra to those obtained by low-energy multiple collision-induced dissociations. Both the PSD experiment with the ref-TOF and the CID experiment with the tandem TOF (applying the bypass option in the AutoSpec-oaTOF) should in principle experience interferences from delayed ionization, as both experiments apply a continuous ion extraction from the source in combination with a pulsed deflection device for the ion separation. Thus, delayed $C_{70}^{+\cdot}$ ions may arrive at the pusher electrode at the same time as the ions of interest such as $C_{132}^{+\cdot}$. The following explanation for the lack of delayed ion signals is proposed. The much greater flight length of the AutoSpec-oa TOF, when compared to the Kompact IV, is of significance; the orthogonal TOF region of the AutoSpec-oa TOF is much further from the ion source than the ion gate on the Kompact IV. Therefore, much greater delay times are required in order for delayed ions to coincide with higher mass ions at the respective reference points which are crucial for the experiment. Neutral species which experience longer delays prior to ionization may leave the ion source with lower kinetic energies. It then follows that the two electrostatic sectors incorporated into the design of the hybrid instrument will “filter out” ions which possess much lower kinetic energies, and such delayed ions will never reach the orthogonal TOF region.

Fig. 9 represents a typical LDI spectrum obtained from a pure $C_{60}$ target, where the data processing parameters are disabled, such as baseline subtraction and smoothing. The spectrum has been recorded in reflectron-mode without the use of the ion gate and features the prominent tailing of the $C_{60}^{+\cdot}$ signal as the result of delayed ionization, which is well known and was exhibited in the original papers detailing delayed ionization as a phenomenon. [29,31] As an example, in relevance to the initial PSD experiments detailed at the beginning of this publication, the delay time required for $C_{60}$ to reach the ion gate at the same

time as $C_{120}$ is labeled on the tail. For an initial velocity of neutrals in the region between 100 and 1000 $ms^{-1}$, a delay time of between 1.1 and 1.2 $\mu$s is required for the delayed $C_{60}^{+\cdot}$ ion to pass the gate at the same time as the dimeric species, $C_{120}^{+\cdot}$. Based on flight time calculations the tail can be estimated to merge with the noise level in Fig. 9 after a delay time of approximately 4 $\mu$s. As mentioned previously, for these instrumental conditions, the extent to which delayed ionization occurs depends on the laser fluence and the fullerene sample used. It should be noted that the observed delay times in experiments involving the ref-TOF mass spectrometer are shorter than those required to cause interferences in the AutoSpec-oaTOF, and that the electrostatic sectors of the latter instrument would need to be scanned in order to observe delayed-ionized species, due to the kinetic energy difference.

## 4. Conclusion

PSD spectra of carbon cluster cations as obtained by the use of a static acceleration voltage and an ion gate for precursor ion selection can exhibit tremendous interefence from fullerenes caused by delayed ionization. The extent to which these interferences can occur depends on several experimental parameters such as the ion source dimensions, the actual position of the ion gate in the flight tube, the translational energy of the ions, the ratio of the mass of the gated ion to the mass of the interfering ion and the extent to which delayed ionization occurs as a function of the fullerene chosen and the ionization method used. These interferences are not restricted to fullerenes, but have to be taken into account whenever ions are formed with a certain delay after the actual excitation event, as for instance observed for certain metallocarbohedrene clusters [44]. Alternatively, the setup utilised in this investigation might represent an interesting alternative to the commonly applied "delayed extraction," in order to deliberately investigate delayed ionization. Experiments to test this are currently being performed in our laboratory.

## Acknowledgements

The authors are thankful to Dr. M.R. Green and Dr. R.H. Bateman (Micromass Ltd., Manchester) for providing access to the AutoSpec-oaTOF. Furthermore, we would like to thank Dr. A.-M. Hoberg and Professsor P.J. Derrick (Warwick) who contributed the results shown in Fig. 2. It is a pleasure to acknowledge many enlightening discussions with Dr. M. Belov, Dr. R. J. Noll, and D. Chrastina. During their visit to Warwick, L. Käseberg (Leipzig) and O. Belgacem (Vienna) helped with some of the experiments at an early stage of this project. Last but not least, this work has been made possible due to the financial support by the EPSRC and The Leverhulme Trust.

## References

[1] B. Spengler, F. Lützenkirchen, S. Metzger, P. Chaurand, R. Kaufmann, W. Jeffrey, M. BartleJones, D.J.C. Pappin, Int. J. Mass Spectrom. Ion Processes 169 (1997) 127.
[2] R. Kaufmann, D. Kirsch, J.L. Tourmann, J. Machold, F. Hucho, Yu. Utkin, V. Tsetlin, Eur. Mass Spectrom. 1 (1995) 313.
[3] B. Spengler, D. Kirsch, R. Kaufmann, Rapid Commun. Mass Spectrom. 5 (1991) 198.
[4] M. Karas, D. Bauchmann, U. Bahr, F. Hillenkamp, Int. J. Mass Spectrom. Ion Processes 78 (1987) 53.
[5] M. Karas, F. Hillenkamp, Anal. Chem. 60 (1988) 2299.
[6] H.W. Kroto, J.R. Heath, S.C.O. O'Brien, R.F. Curl, R.E. Smalley, Nature 318 (1985) 162.
[7] C. Yeretzian, K. Hansen, F. Diedrich, R.L. Whetten, Nature 359 (1992) 44.
[8] B. Kubler, E. Millon, J.J. Gaumet, J.F. Muller, Fullerene Sci. Technol. 4 (1996) 1247.
[9] Z.-Y. Liu, C.-R. Wang, R.-B. Huang, L.-S. Zheng, Int. J. Mass Spectrom. Ion Processes 145 (1995) 1.
[10] A.A. Shvartsburg, G.C. Schatz, M.F. Jarrold, J. Chem. Phys. 108 (1998) 2416.
[11] P. Dugourd, R.R. Hudgins, J.M. Tenenbaum, M.F. Jarrold, Phys. Rev. Lett. 80 (1998) 4197.
[12] G. von Helden, M.T. Hsu, N. Gotts, M.T. Bowers, J. Phys. Chem. 97 (1993) 8182.
[13] G. von Helden, M.T. Hsu, P.R. Kemper, M.T. Bowers, J. Chem. Phys. 95 (1991) 3835.
[14] R. Cozzolino, O. Belgachem, T. Drewello, L. Käseberg, R. Herzschuh, S. Suslov, O. V. Boltalina, Eur. Mass Spectrom. 3 (1997) 407.
[15] P.P. Ong, L. Zhu, L. Zhao, J. Zhang, S. Wang, Y. Li, R. Cai, Z. Huang, Int. J. Mass Spectrom. Ion Processes 163 (1997) 19.

[16] R. D. Beck, P. Weis, A. Hirsch, I.J. Lamparth, J. Phys. Chem. 98 (1994) 9683.
[17] R.D. Beck, C. Stoermer, C. Schulz, R. Michel, P. Weis, G. Bräuchle, M.M. Kappes, J. Chem. Phys. 101 (1994) 3243.
[18] R.D. Beck, P. Weis, J. Rockenberger, M.M. Kappes, Surf. Rev. Lett. 3 (1996) 771.
[19] R.D. Beck, P. Weis, G. Bräuchle, M.M. Kappes, J. Chem. Phys. 100 (1994) 262.
[20] U.N. Andersen, A.W. Colburn, A.A. Makarov, E.N. Raptkis, D.J. Reynolds, P.J. Derrick, S.C. Davis, A.D. Hoffman, S. Thomson, Rev. Sci. Instrum. 69 (1998) 1650.
[21] M.M. Cordero, T.J. Cornish, R.J. Cotter, J. Am. Soc. Mass Spectrom. 7 (1996) 590.
[22] M.P. Barrow, J.K. Cammack, M. Goebel, I.M. Wasser, K.P.C. Vollhardt, T. Drewello, J. Organomet. Chem. 572 (1999) 135.
[23] M.P. Barrow, N.J. Tower, R. Taylor, T. Drewello, Chem. Phys. Lett. 293 (1998) 302.
[24] M.M. Cordero, T.J. Cornish, R.J. Cotter, I.A. Lys, Rapid Commun. Mass Spectrom. 9 (1995) 1356.
[25] H. Hohmann, C. Callegari, S. Furrer, D. Grosenick, E.E.B. Campbell, I.V. Hertel, Phys. Rev. Lett. 73 (1994) 1919.
[26] M. Foltin, O. Echt, P. Scheier, B. Dunser, R. Wörgötter, D. Muigg, S. Matt, T.D. Märk, J. Chem. Phys. 107 (1997) 6246.
[27] R. Mitzner, B. Winter, C. Kusch, E.E.B. Campbell, I.V. Hertel, Z. Phys. D 37 (1996) 89.
[28] A.A. Shvartsburg, R.R. Hudgins, P. Dugourd, M.F. Jarrold, J. Phys. Chem. A 1001 (1997) 1684.
[29] E.E.B. Campbell, G. Ulmer, I.V. Hertel, Phys. Rev. Lett. 67 (1991) 1986.
[30] E.E.B. Campbell, G. Ulmer, I.V. Hertel, Z. Phys. D 24 (1992) 81.
[31] P. Wurz, K.R. Lykke, J. Chem. Phys. 95 (1991) 7008.
[32] P. Wurz, K.R. Lykke, J. Phys. Chem. 96 (1992) 10129.
[33] A.C. Jones, M.J. Dale, M.R, Banks, I. Gosney, P.R.R. Langridge-Smith, Mol. Phys. 80 (1993) 583.
[34] D. Ding, R.N. Compton, R. Haufler, C.E. Klots, J. Phys. Chem. 97 (1993) 2500.
[35] D. Ding, J. Huang, R.N. Compton, C.E. Klots, R. Haufler, Phys. Rev. Lett. 73 (1994) 1084.
[36] K. Hansen, O. Echt, Phys. Rev. Lett. 78 (1997) 2337.
[37] R. Deng, O. Echt, J. Phys. Chem. A 102 (1998) 2533.
[38] P. Juhasz, M.L. Veatal, S.A. Martin, J. Am. Soc. Mass Spectrom. 8 (1997) 209.
[39] T.-W.D. Chan, I. Thomas. A.W. Colburn, P.J. Derrick, Chem. Phys. Lett. 222 (1994) 579.
[40] R.H. Bateman, M.R. Green, G. Scott, E. Clayton, Rapid Commun. Mass Spectrom. 9 (1995) 1227.
[41] M.P. Barrow, H. Hungerbühler, K.-D. Asmus, M.R. Green, R.H. Bateman, T. Drewello, unpublished.
[42] J. Byun, J. Gooden, R. Ramanthan, K.-M. Li, E.L. Cavalieri, M.L. Gross, J. Am. Soc. Mass Spectrom. 8 (1997) 977.
[43] X. Zhang, J. JaiNhuknan, C.J. Cassady, Int. J. Mass Spectrom. Ion Processes 171 (1997) 135.
[44] S.F. Cartier, B.D. May, A.W. Castleman, J. Chem. Phys. 104 (1996) 3423.